Original Article

Hydraulic modeling of submerged seawalls under high-velocity tsunami currents

[1)]Igarashi Kogyo Co. Ltd. Chiba City, Chiba Prefecture, 261-0002 Japan
[2)]PC depo-smart life, Kitano 2-5-33, Mitaka city, Tokyo 181-0003, Japan
[3)]Institute of Environmental Biology, Kyowa-Kako, Tadao2-15-5, Machida City, Tokyo 194-0035 Japan

Atsushige Tanaka[1)] , Eisaburo Matsunaga[1)] , Rina Kohata[2)] , Yasuhiro Yoshikawa[3)]

Summary On March 11, 2011, the Great East Japan Earthquake (GEJE) generated one of the most destructive tsunamis in history. A portion of the tsunami propagated southward off Kashimanada, Ibaraki Prefecture, passed the mouth of the Tone River, and sharply deflected toward the Choshi coast in Chiba Prefecture, traveling along the cliffs of Byobugaura.

During field observations from a hillside overlooking the Marina coast, we recorded a stationary "giant white wall of water" (GW3) offshore, followed by a dull copper-colored beneath-jet current (BeJeC) that overtook the preceding surface wave flow (SuWaF). This striking scene indicated that the BeJeC, rather than the surface wave, carried the primary destructive force.

To evaluate possible countermeasures, we analyzed the SuWaF–BeJeC structure and conducted high-velocity tsunami-mimic circulating flume tank (T-mCFT) experiments with duct-type and perforated-plate-type submerged seawall models. These experiments showed that the structures induced significant backflow, amounting to roughly half of the incoming flow volume.

Numerical extrapolation, combining field-based tsunami models with experimental data suggesting a potential reduction of 65-75% in specific forces under the model conditions, indicating that submerged seawalls substantially decrease run-up height. These findings support the practical effectiveness of submerged seawalls as a countermeasure against mega- tsunamis.

Key words: Great East Japan Earthquake (GEJE), submerged seawall, giant white wall (GW3), surface wave flow, beneath-jet current, tsunami-mimic circulating flume tank

*Correspondence to: Yoshikawa, Y.: y-yoshikawa@ous.ac.jp
Received 16 December 2025; Accepted 25 February 2026

Introduction

The 2011 Great East Japan Earthquake (GEJE) generated an unprecedented tsunami that caused catastrophic destruction along the Tohoku coastline. Although the ground shaking was strong, it consisted of extremely long-period lateral motions; thus, structural damage to buildings remained relatively limit-ed. In contrast, the accompanying tsunami exhibit-ed overwhelming destructive power. In Miyako City, Iwate Prefecture, run-up heights exceeded 37 m, among the highest ever recorded worldwide. In Kesennuma and Minamisanriku, entire urban dis-tricts were devastated, while powerful return flows in Onagawa displaced even multi-story reinforced concrete buildings. These examples highlight the extraordinary destructive capacity of tsunami cur-rents, both in inflow and return phases.

On the same day, a massive tsunami struck Choshi City, Chiba Prefecture, where our research base is located. From a hillside overlooking the Marina coast, we observed a stationary giant white wall of water (hereafter referred to as GW3) offshore. Then, beneath-jet current (BeJeC) appearing a dull copper-colored due to suspended sediment and light reflection overtook the preceding surface wave flow (SuWaF). Unlike the SuWaF, which mainly produced surface undulations, the BeJeC advanced as a destructive supercritical jet, colliding with coastal reefs and overtopping massive rock formations. These field observations indicated that the BeJeC was the primary destructive component of the tsunami.

Following the 2011 disaster, many studies advanced our understanding of tsunami generation, propagation, and impacts. Tsunami waveform inversion studies clarified coseismic slip distributions[1], while integrated geodetic and waveform analyses produced refined fault source models[2]. Numerical simulations have estimated damage and casualties[3], and observation results and large-scale water tank experiments etc. revealed mechanisms of coastal dike failures[4,5]. Reviews have further synthesized advances in physical modeling[6]. However, conven-tional countermeasures such as tall breakwaters, though effective against surface waves, are not well suited to resisting high-velocity jet-like flows such as the BeJeC.

In contrast, natural porous barriers − particularly coral reefs—have demonstrated the ability to dissipate tsunami energy by inducing drag, turbulence, and backflow. Observational and experimental studies have shown that reef roughness can reduce flow velocity and energy flux, thereby mitigating run-up[7,8,9]. Inspired by these natural defenses, we explored whether engineered submerged seawalls could reproduce similar effects.

Building on our field observations in Choshi, we developed experimental models of duct-type and perforated-plate-type submerged seawalls using a high-velocity tsunami-mimic circulating flume tank (T-mCFT). Installed in tandem, these models induced controlled backflow that reduced tsunami energy. The present study reports on these experiments, quantitative analyses, and extrapolated simulations, and proposes submerged seawalls as a new countermeasure against destructive tsunami jet currents.

Field observation of the tsunami: structure and characteristics of tsunami flows

Around noon on March 11, 2011, the GEJE and the accompanying tsunami reached the offshore area in front of the Marina coast of Choshi City, Chiba Prefecture, where the massive cliffs of Byobugaura rise. At that time, our research group had been conducting flume experiments nearby but immediately halted the T-mCFT study and joined the evacuation of residents and workers toward designated high-ground sites.

From the observation point known as “Hill Where You Can See the Round Earth Park,” we had an unobstructed view of the coastline. About one-kilometer offshore, a towering GW3, approximately 10 m high and 30–50 m wide, appeared almost stationary, with little horizontal displacement. A faint white mist hovered above it, indicating strong entrainment of air and spray. Shortly afterward, from beneath GW3, a powerful BeJeC surfaced and advanced as a broad, flat jet-like flow. Its surface

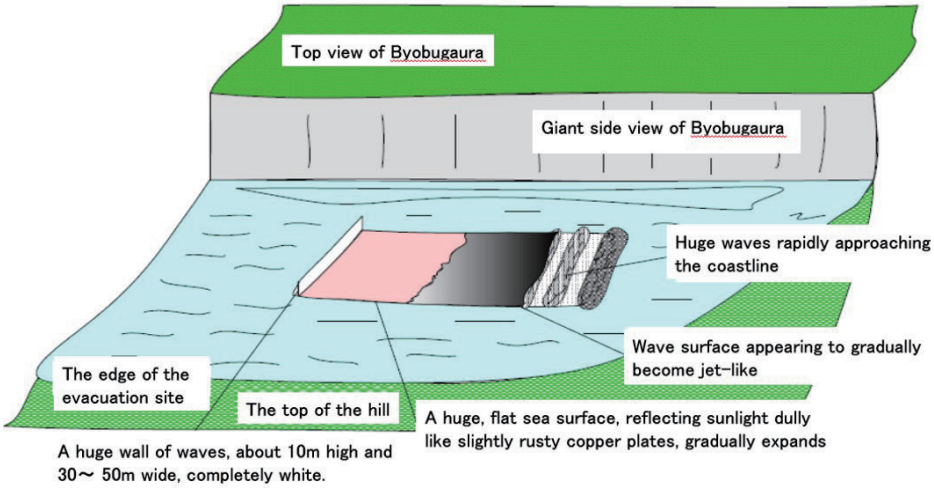

Fig. 1 Schematic illustration of the tsunami observed off the Marina coast during the 2011 GEJE
The GW3, approximately 10 m high and 30– 50 m wide, appeared nearly stationary offshore. Beneath it, the BeJeC advanced with a flat copper-hued surface. The diagram also shows the relative positions of the Byobugaura cliffs, the elevated evacuation site, and the observed flow features.

reflected sunlight in a dull copper hue, a striking visual feature that distinguished it clearly from the preceding SuWaF (Fig.1).

From this vantage point, we could simultaneously recognize multiple flow components: stationary GW3, the BeJeC with its copper-toned flat surface, smaller preceding SuWaF ripples, and farther offshore, larger turbulent waves were progressing toward the coast. To the south, another GW3 formed, under which a second BeJeC began to emerge. These ob-servations provided the first compelling evidence that the tsunami consisted of dual structures-SuWaF and BeJeC-with the latter carrying the principal de-structive force.

Impact of the massive tsunami near residential areas

In Japan, it is well recognized that massive tsunamis strike coastal regions once every few hundred years, yet their precise timing cannot be predicted. On March 11, 2011, the tsunami generated by the GEJE advanced into the shallow sea off Choshi, Chiba Prefecture. After passing through Inubosaki, which extends north–south across the Tone River from Kashimaura in Ibaraki Prefecture, the currents entered the broad Byobugaura embayment stretching east–west from Tagawa to Gyobu Misaki. The tsunami gradually propagated across this shallow sea, traveling along the towering rock formations of Byobugaura before surging across the coastline and running up onto the land.

Fig. 2a presents a bird's-eye view of the residential areas and university facilities situated just inland of Choshi Marina, directly exposed to the advancing flows of the SuWaF and BeJeC. Fig. 2b depicts the southern face of a massive Byobugaura rock formation, which was severely eroded and collapsed under the force of the tsunami. Fig. 2c shows the interior of Café Marina, where the incoming flow lifted a car diagonally toward the ceiling before it eventually crashed down. The initial SuWaF veered slightly to the right, striking a hillside snack shop and the university guard station, while the BeJeC continued directly forward, leaving impact marks on the lower walls of university buildings situated on slightly elevated ground.

A contemporaneous newspaper article recorded an additional incident. Firefighters had guided residents from near the coast to higher ground. After completing the evacuation, one firefighter attempted to close a protective gate installed on a narrow slope to prevent tsunami inflow up a mountain path. As the massive wave was already approaching, he only managed to partially close the gate before escaping. Remarkably, inspection on the following day revealed that the gate had functioned as if fully

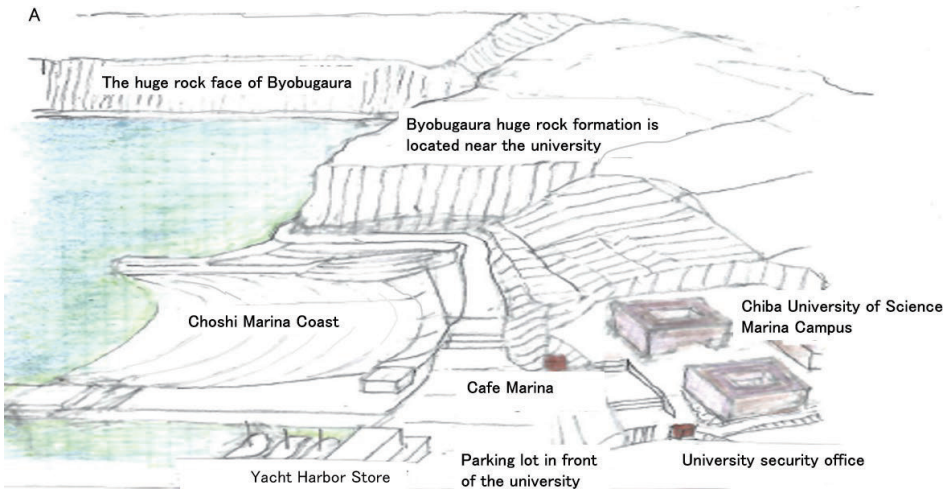

Fig. 2 Bird's-eye view of the residential area and university facilities
(A) They are located behind Choshi Marina Coast, where the SuWaF and BeJeC struck in succession.

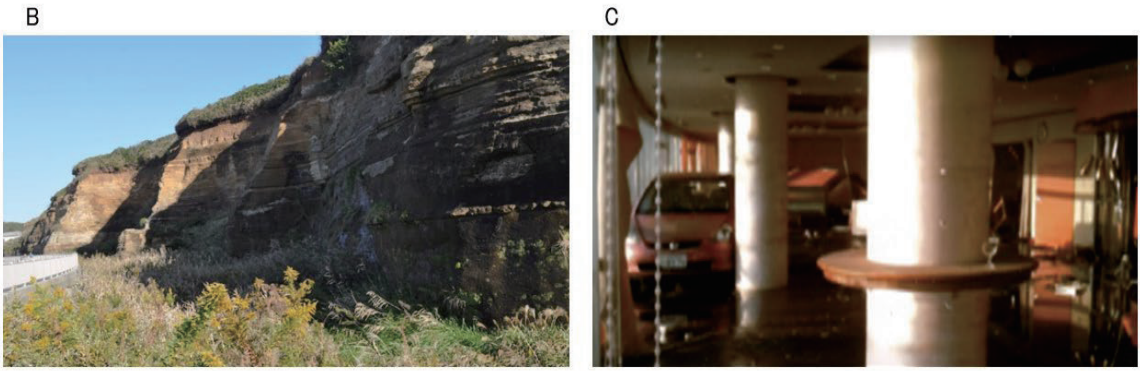

Fig. 2 Remains of the massive Byobugaura rock formation and Café Marina
(B) The rock where the southern face was severely eroded and collapsed by the tsunami.
(C) Interior of Café Marina, where a car lifted diagonally upward toward the ceiling by the tsunami wave flow eventually fell.

closed, successfully blocking the advance of the tsunami. This episode suggested that barriers with perforations-similar in principle to porous plates-might exert significant protective effects against the destructive BeJeC, in contrast to the more moderate SuWaF.

Characteristics and Structure of Giant Tsunamis

On the sea surface, a GW3 suddenly appeared, followed by a SuWaF. Shortly thereafter, a BeJeC spread forward across the sea surface in front of the wall. To interpret these observations quantitatively, we estimated the height of the GW3, the height of the SuWaF flowing over the quasi-stationary surface, and the velocity of the tsunami current traveling across the sloping seabed. These parameters were then used to calculate tsunami heights, flow velocities, and inundation levels at the coastline.

Fig. 3a–c illustrates the positions of the sea edge, midpoint, and coastline, plotted as horizontal distance (x, km) against seafloor depth (y, m). The propagation of the SuWaF near the sea edge, and the BeJeC rising from the seabed to overtake the SuWaF, are shown in Fig. 3c. To describe these flows, both mass conservation and momentum conservation equations were applied separately to the oscillatory SuWaF and to the jet-like BeJeC.

For the SuWaF (water depth hs, velocity us), the continuity equation is expressed as:

$\partial (\rho hsus) / \partial x = 0$, and the momentum conservation as: $\partial (\rho hsus^2) / \partial x = \partial (\rho hsg (hs + hb)) / \partial x$ where ρ is density, and hb represents the depth of the underlying jet flow. These equa-tions

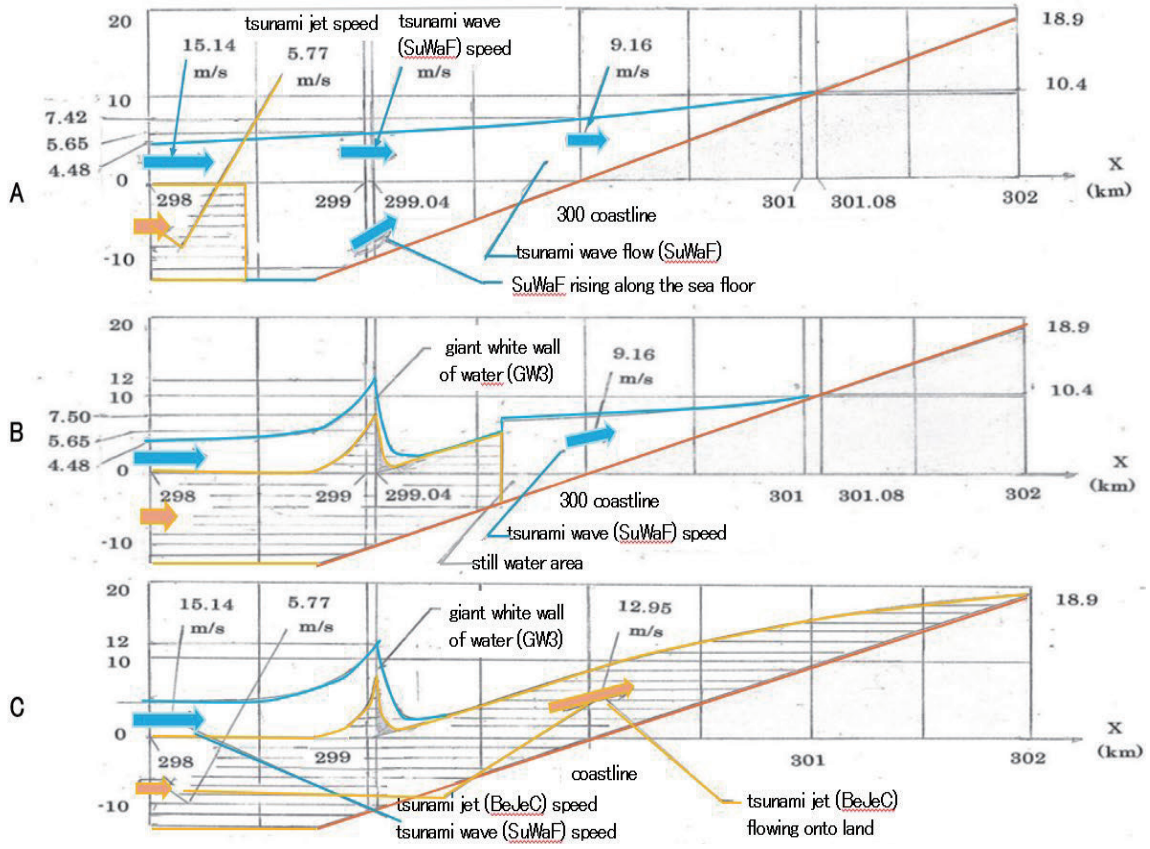

Fig. 3 Structure of the tsunami approaching land and the GW3 emergence.
(A) SuWaF propagating toward the coastline and decelerating nearshore.
(B) BeJeC overtook the SuWaF and formed a ~12 m GW3 before striking coastal reefs.
(C) BeJeC surging inland with a maximum velocity of 12.95 m/s and water level reaching 18.9m, approximately 2 km from the coastline.

show that the SuWaF conserves its discharge while being dynamically influenced by the BeJeC beneath it.

For the BeJeC (water depth hb, velocity ub), the continuity equation is:

$\partial(\rho\, hbub)/\partial x = 0$, and the momentum conservation is:

$\partial(\rho\, hbub^2)/\partial x = \partial(\rho\, hsghb)/\partial x$ indicating that the BeJeC can be interpreted as being influenced by the pressure gradient associated with the overlying SuWaF. In other words, the BeJeC accelerates as a rising water mass powered by the level difference created by the SuWaF.

The epicenter of the GEJE was located off the Oshika Peninsula, Miyagi Prefecture (38° 06.2′ N, 142° 51.6′ E), at a depth of 24 km, approximately 300 km from Choshi City. The SuWaF propagated rapidly in the upper layer, traveling at ~15.1 m/s at 2 km offshore and decelerating to ~9.2 m/s near the coastline. The wave height was ~7.4 m and reached~10.4 m at 1 km inland.

The BeJeC appeared about 1 km offshore, overtook the SuWaF, and lifted it to form the GW3, reaching a height of ~12 m. It then advanced almost linearly, colliding with massive reefs and overtopping rock formations before surging inland at ~12.9 m/s. At ~2 km inland, the maximum water level reached ~18.9 m.

From these results, the SuWaF can be interpreted as producing water-level fluctuations and modest surface velocities, exerting limited destructive force as push-and-pull waves. By contrast, the BeJeC exhibited supercritical flow (Froude number > 1), advancing as a wall-like current exceeding 10 m/s. This jet-like component was responsible for most of the destructive impacts on houses, forests, and infrastructure.

Based on these observations and the identified

flow structure, we subsequently carried out T-mCFT experiments to evaluate whether submerged seawalls could mitigate the destructive forces of tsunami currents.

High-velocity circulating flume tank for tsunami simulation (T-mCFT)

The structural configuration of the high-velocity T-mCFT used in this study is shown in Fig. 4a. The tank measures 10.1 m in length, 3.0 m in width, and 2.1 m in height, with a total water capacity of 150 t. It is equipped with a bubble-removal unit and a sediment/gravel collection device. To suppress surge flow defined here as a sudden rise in water level or unstable oscillatory motion, an auxiliary surge-avoidance tank (0.8 m × 0.4 m × 0.4 m) was integrated into the system.

The measurement section (Fig. 4b), 3.5 m in length, 0.5 m in width, and 0.6 m in water depth, was designed to reproduce the characteristics of large-scale, high-velocity tsunami-like flows with high fidelity. Prior to each experiment, a U-shaped rubber nozzle was installed at the rear upper part of the section, allowing incoming water to accumulate upstream and form a mound. Once sufficiently developed, this mound generated a new high-velocity current, providing stable and reproducible conditions for investigating tsunami flows.

The flow regime was evaluated using Reynolds number (Re) and Froude number (Fr), confirming fully turbulent supercritical conditions. To avoid uncontrolled surge flow typically observed at Froude numbers ≥ 2.0, the measurement section was constructed as a dual-layer channel, with the lower layer serving for surge suppression. Since the setup employed high-velocity tsunami flows Fr ≥

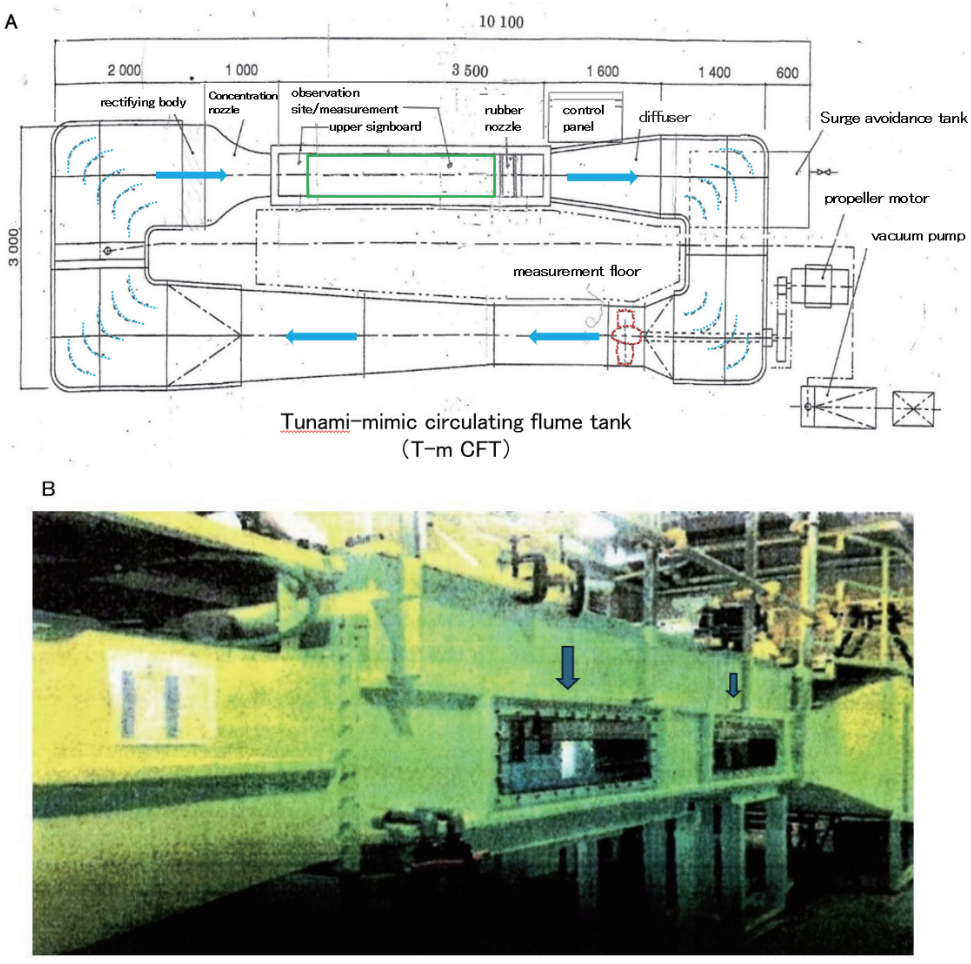

Fig.4 Structure configuration and measurement section of T-mCFT
(A) Plan view of the high-velocity T-mCFT.
(B) Measurement section (arrowheads) of the T-mCFT.

2.0 (supercritical jet regime), a simple widening of the channel would have induced re-transition into jet flow. Instead, the section was extended to 3.5 m, enabling the maintenance of a stable constant flow. A large upstream reservoir was also placed ahead of the duct and propeller system to damp turbulence and sustain steady velocities.

In the experiments, a duct-type submerged seawall model was installed at the upstream end of the measurement section to convert incoming jet flow (Fr ≥ 2.0) into less destructive subcritical flow. However, the flow re-transitioned into a jet (Fr ≈ 1.5) downstream, which was then passed through a perforated-plate-type submerged seawall model. Precision glass windows along the sidewalls of the section allowed direct observation of the flow patterns.

For performance evaluation, the duct-type seawall was consistently placed upstream and the perforated-plate-type seawall downstream, enabling assessment of the combined reduction effect of paired models. To further prevent large-scale backflow generated by the seawalls, the flume was designed as a two-layer structure consisting of the main experimental flow path and an auxiliary backflow-prevention path.

Experiments using model seawall devices in the T-mCFT

To investigate the effectiveness of submerged seawalls in mitigating tsunami forces, we constructed two model devices: a duct-type seawall and a perforated-plate-type seawall (Fig. 5a, b). Both models measured 0.1 m in height, 0.4 m in length, and 0.3 m in width, corresponding to scaled conditions of shallow-sea installations. The duct-type model consisted of two parallel flow channels, while the perforated-plate-type model had outer walls perforated on its upper and lateral faces.

When placed in the T-mCFT, both models induced partial backflow and turbulence, thereby reducing the momentum of the jet-like tsunami flow. Fig. 6a and 6b illustrate typical flow patterns: in the duct-type model, the incoming jet separated into forward flow and strong upstream-directed backflow, whereas in the perforated-plate-type model, water penetrated through the perforations while generating weaker but distributed backflow. In both cases, the jet flow was broken down into multiple velocity layers (surface, middle, and bottom), which significantly altered downstream flow structure.

The evaluation of the duct-type and perforated-

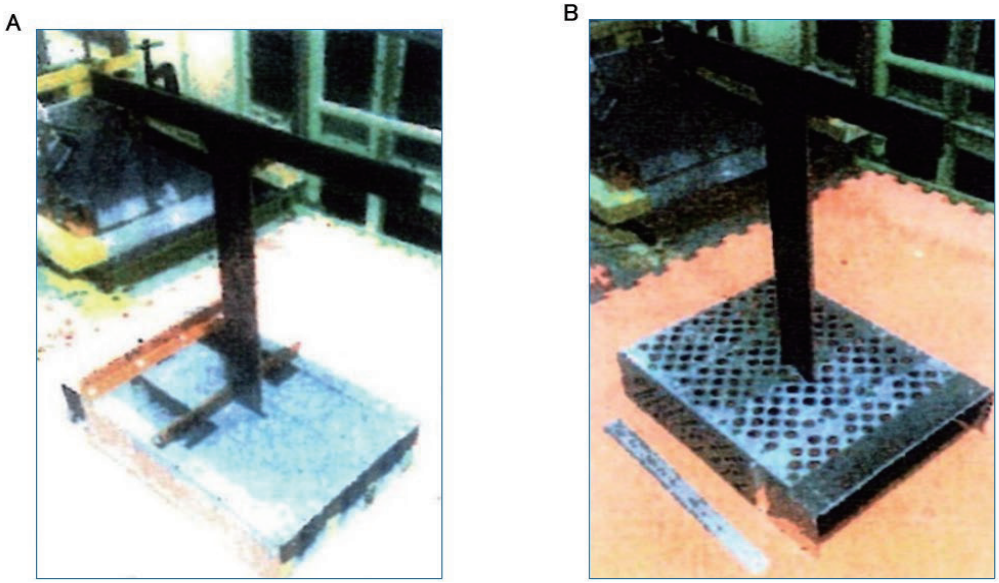

Fig. 5 Two submerged seawall models used in the T-mCFT experiment
(A) Duct-type seawall model and (B) perforated-plate-type seawall model.

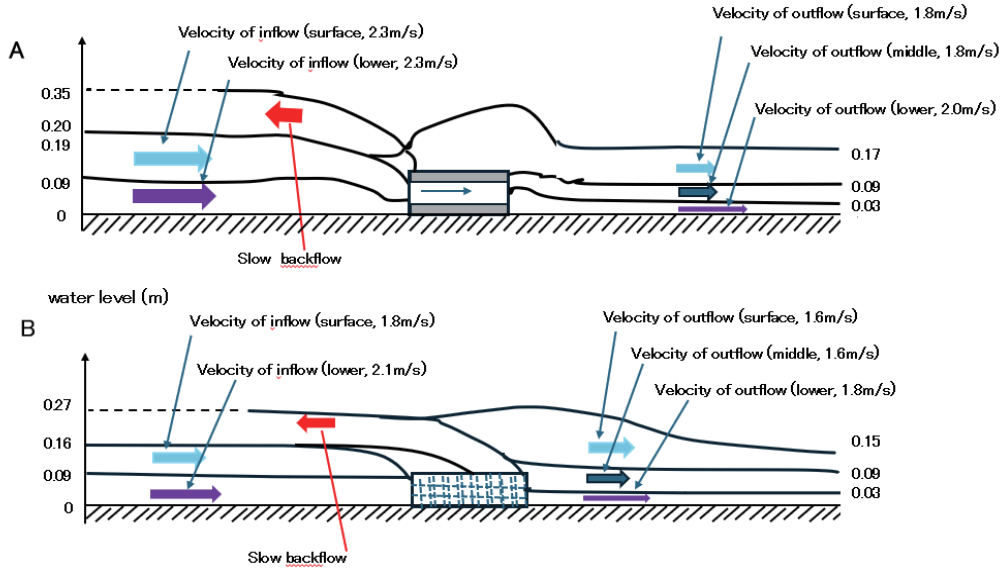

Fig.6 Flow patterns of two submerged seawall models
(A) Flow patterns with duct-type and (B) perforated-plate-type seawalls, showing separation into forward flow (blue, purple) and induced backflow (red).

plate-type models was intentionally developed step by step, to highlight their function as "energy-reducing porous barriers," analogous to coral reefs. Rather than stopping the jet flow completely, these devices promote turbulence and backflow that redistribute and dissipate momentum.

We first examined continuity of discharge. For the duct-type model (Fig. 6a), the inflow discharge was given by dWqi= (0.10 × 2.3) +(0.09 × 2.3) =0.437 m^2/s,

while the outlet discharge was dWqo= (0.03 × 2.0) +(0.06 × 1.8) +(0.08 × 1.8) =0.312 m^2/s. The difference represents the upstream-directed return flow, which, for an effective backflow depth of 0.15 m, yields a velocity of ubf= − (dWqi − dWqo)/ 0.15= − 0.83 m/s.

Building upon this, we next introduced the specific force, $M=\Sigma(hiui^2+(1/2)\ ghi^2)$,

which combines momentum flux and hydrostatic pressure. At the duct inlet (hi=0.19m, ui=2.3 m/s), Min=1.09 m^3/s^2, while at the outlet, Mout=0.63 m^3/s^2. Thus, 0.47 m^3/s^2 (43%) of the incident specific force was redirected upstream.

Applying the same procedure to the perforated-plate-type model (Fig. 6b), the backflow velocity was − 0.63 m/s. The inlet and outlet specific forces were 0.69 and 0.44 m^3/s^2, respectively, resulting in a backflow component of 0.24 m^3/s^2 (35%). Finally, when the two devices were installed in series, the combined backflow force amounted to 0.71 m^3/s^2, equivalent to a 0.71/1.093=0.65, 65% reduction of the incident jet momentum.

Effects of combining a duct-type and a perforated-plate-type seawall model device

To examine the reduction of jet flow destructive power by a double submerged seawall system, a duct-type seawall model was placed upstream and a perforated-plate-type model downstream, separated by a prescribed interval, within the T-mCFT. Fig. 7a illustrates the setup under still-water conditions, while Fig. 7b shows the system under high-velocity jet flow.

Under flow conditions, the backflow accompanied by foaming consisted of two distinct components: one with strong momentum originating from the duct-type model, and another with slightly weaker momentum generated by the perforated-plate-type model. These two backflows occurred at nearly the same height and maintained considerable velocity, thereby dissipating the energy of the incoming jet. This indicates that combining the two submerged seawall types significantly contributes to mitigating the destructive force of tsunami Be-

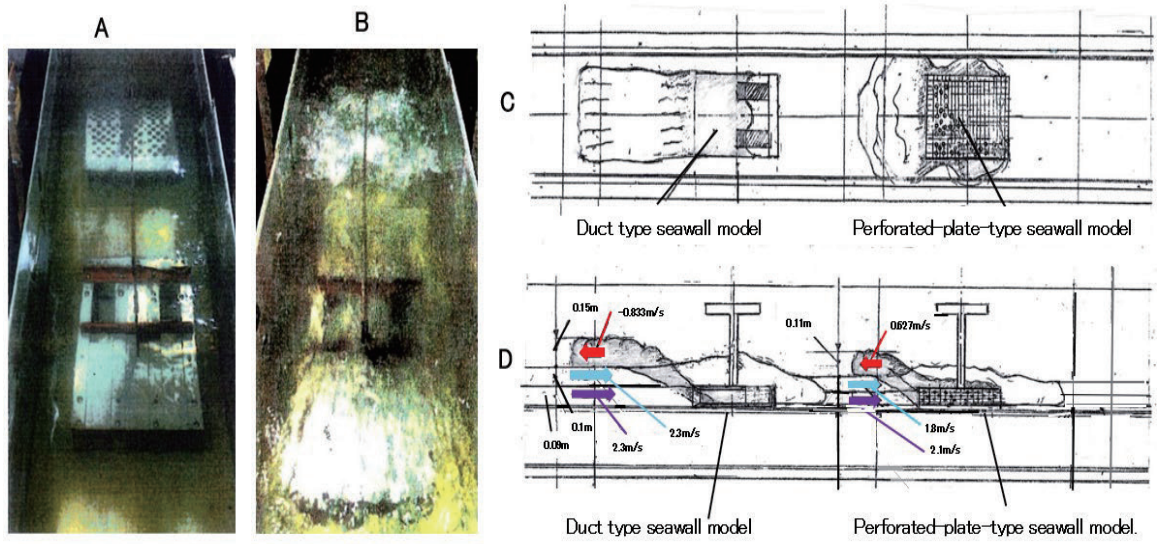

Fig. 7 Duct-type and perforated-plate-type model device installed
(A) still-water conditions; (B) foaming backflow under jet flow; (C) a top view of the two model seawalls; and (D) a side view showing the backflow pattern and the measured water depth (m) and velocity (m/s) of the jet entering each model.

JeC impacting the coastline.

The jet current entered the hollow duct (height: 0.10 m; width: 0.08 m; length: 0.40 m; lateral pillar width: 0.03 m), where it temporarily transitioned into subcritical flow and advanced straight ahead. Near the duct outlet, the flow decelerated and initiated backflow toward the inlet, with no visually detectable discharge of backflow downstream at this stage.

Representative values were derived from the means of multiple experimental runs (Table 1). The total inflow at the duct-type model entrance was: dih × div= 0.19 × 2.3= 0.437 m^2/s. The backflow volume at the duct-type model was: (inflow) − (outflow)= 0.437 − 0.312=0.125 m^2/s, consistent with direct measurement: dbh × ubf= 0.15 × 0.833= 0.125 m^2/s. Thus, the backflow-to-inflow ratio was 0.125 / 0.437 = 0.286 (28.6%).

For the perforated-plate-type model, the inflow was 0.312 m^2/s and the outflow 0.246 m^2/s, yielding a backflow of 0.066 m^2/s. The ratio of backflow to inflow was therefore 0.066 / 0.312 = 0.212 (21.2%). The measured value gave: pbh × ubf=0.11 × 0.627=0.069 m^2/s, equivalent to 22.1%.

From these results, it can be inferred that approximately 50% of the jet current's destructive power is dissipated in the vicinity of the submerged seawalls (Table 1). Taken together, these experi-

Table 1 Backflow volumes used by submerged seawall models in T-mCFT experiments

	Water depth h(m)	Velocity u(m/s)	Flow volume hu(m^2/s)	Total flow volume hu(m^2/s)	Backflow volume hu(m^2/s)
Duct-in	0.09	2.3	0.207	0.437	
	0.10	2.3	0.23		
Duct backflow					0.125 (28.6%)
Duct-out	0.08 (up)	1.8	0.144	0.312	
Pore-in	0.06 (mid)	1.8	0.108		
	0.03 (low)	2.0	0.060		
Pore backflow					0.066 (21.2%)
Pore-out	0.6	1.6	0.096	0.246	
	0.6	1.6	0.096		
	0.3	1.8	0.054		

mental findings provide the quantitative basis for the following simulation analysis, where the effectiveness of combined seawall structures under varying tsunami flow conditions is further examined.

Numerical simulation of the effect of submerged seawalls against tsunami BeJeC

As described earlier, the massive tsunami generated by the GEJE struck the shallow coastal zone of Byobugaura, Choshi City. The current, containing abundant bubbles, vortices, and surface undulations, eventually formed a towering GW3 approximately 10 m in height. From beneath this surge, a high-velocity BeJeC emerged, maintaining a mirror-like sea surface as it advanced toward the shoreline.

In the model experiment, the tsunami's velocity, depth, destructive force, and duration were determined with reference to this event. Because examples of submerged seawalls are extremely limited, and experimental cases of jet-like tsunami flows are even rarer-the model was designed such that a continuous jet flow could strike the seawall device for about one hour to obtain stable statistic averages rather than to replicate real tsunami duration.

The placement, length, spacing, depth, and flow velocity of the duct-type and perforated-plate-type submerged seawall models were set to deflect roughly half of the incoming tsunami current back toward the sea. Installed at a seabed depth of about 5 m and measuring 7-10 m in length, the double submerged seawall system induces gradual return flows before the jet current reaches the seaward ends of the structure.

Within the duct section, the incoming jet turns back toward the inlet, dividing into two components: (1) a steady counter-current flowing along the surface of the incoming current, and (2) a flow rising along the front surface of the seawall and continuing over its top. The flow balance around the structures is summarized in Table 2.

At the duct-type seawall entrance, the total inflow was 86.7 m^2/s. The backflow volume was Inlet– Outlet =86.7-61.9= 24.8 m^2/s, corresponding to 28.3% of the inflow. For the perforated-plate-type seawall, the inflow was 61.9 m^2/s, the backflow volume Inlet-Outlet= 61.9 – 29.3=32.6 m^2/s, corresponding to 37.5%. These results indicate that approximately 66% of the tsunami's destructive flow volume is redirected seaward by the combined structures.

The same trend was confirmed by specific force calculations using $M=hu^2+(1/2)\,gh^2$.

At the duct-type entrance, the specific force was $dMi=6.8\times12.75^2+(9.8\times6.8^2/2)=1332 m^3/s^2$. At the duct outlet, $dMo=589.5 m^3/s^2$ yielding a back-flow

Table 2 Flow and specific force balance around submerged seawall models.

	Water depth (m)	velocity (m/s)	Flow volume (m^2/s)	Total flow (m^2/s)	Specific force (m^3/s^2)	Note
SuWaF BeJeC	4.48 10.0	15.14 5.77	67.8 57.7	125.5	1948.1	
GW3 emergence					-616.1	1948.1-1332
Duct-in	6.8	12.75	86.7	86.7	1332.0	
Duct backflow				24.8 28.3%	-742.5 55.7%	1332-589.5
Duct-out Pore-in	up 3.2 mid 2.4 low 1.2	8.8 9.2 9.7	28.2 22.1 11.6	61.9	589.5	
Pore backflow				32.5 37.5%	-293.6 22.0%	589.5-295.9
Pore-out	up1.8 mid 1.8 low 0.9	7.9 7.4 7.4	14.2 8.5 6.7	29.3	295.9	
Upstream jet no seawalls	6. 8	12.95	88.1	88.1	1367	18.9m upstream height
Upstream jet with seawalls	mid 1.8	7.4	12.3	12.3	114.4	1.58m upstream height

specific force of

dMb=dMi − dMo=742.5m^3/s^2 (55.7%). For the perforated-plate-type seawall, the outlet is pMo=295.9m^3/s^2, and the backflow specific force was pMb=dMo; pMi − pMo=293.6m^3/s^2.

Thus, the combined backflow specific force was (dMb+pMb)/dMi= (742.5+293.6)/1332=0.778, indicating that a substantial portion of the incoming tsunami energy is dissipated by the double submerged seawalls (Fig. 8a).

Thus, large-scale backflows generated by the submerged seawalls are expected to significantly reduce the destructive energy of tsunami currents approaching the coast. While part of the flow continues forward as a straight jet, its impact is diminished. Without seawalls, the upstream specific force is 1367 m^3/s^2, however, with seawalls, the specific force becomes 114.4 m^3/s^2. Therefore, the upstream height in the latter case is estimated as (18.9 × 114.4) / 1367 = 1.58 m. The residual jet flow is estimated to run up inland to a height of only about 1.6 m (Fig. 8b).

In addition to these structural effects, the tsunami itself undergoes a major transformation during its inland advance. Before the BeJeC overtakes the SuWaF, a large mound of water (GW3) develops. The formation and collapse of this GW3 consumes a considerable portion of the tsunami' s energy. The specific force of tsunami flow before GW3 is 1948,1m^3/s^2 and after GW3 is 1332m^3/s^2, thus 616.1m^3/s^2 is lost. From the perspective of energy dispersion, this natural transformation of the flow

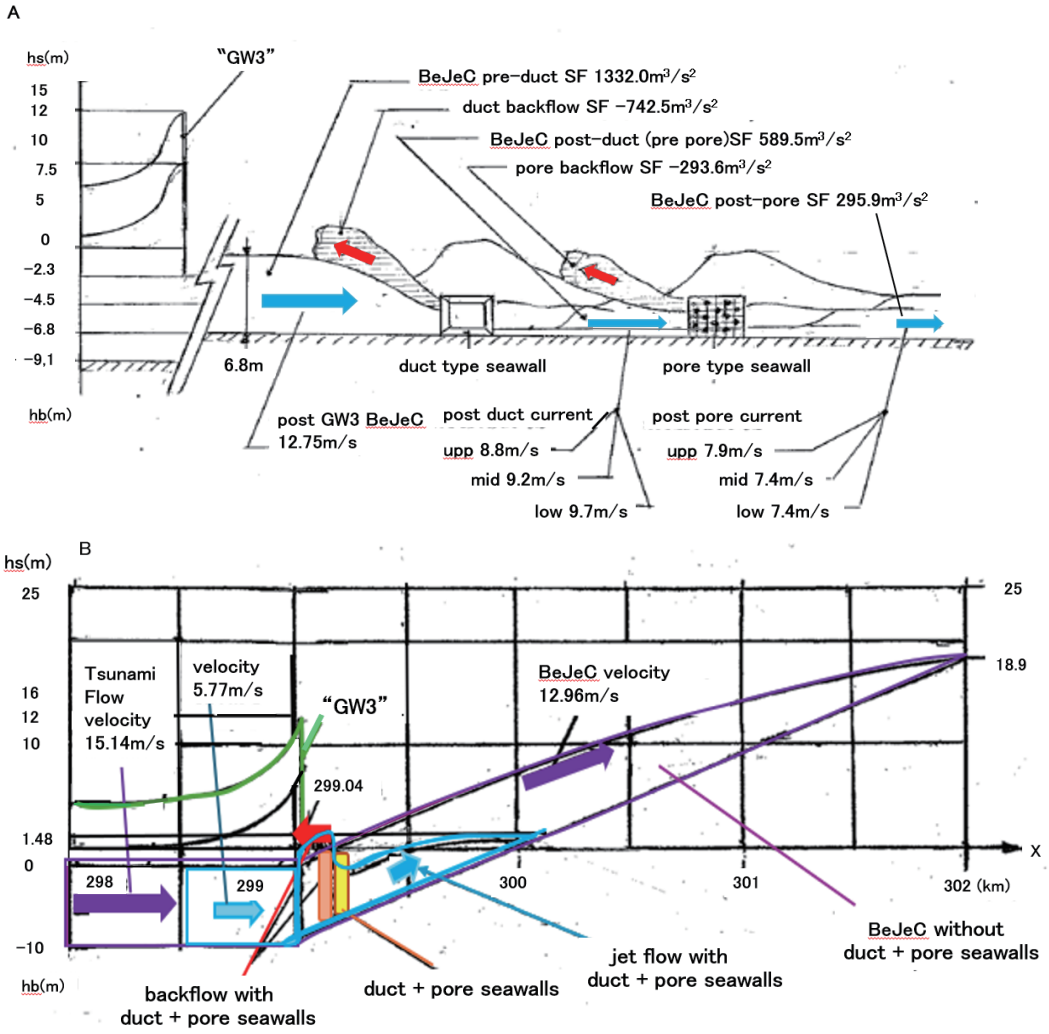

Fig. 8 Simulation of the tsunami flow with GW3 and jet flow
(A) Scheme of the tsunami flow producing GW3 and subsequent jet flow.
(B) Height of BeJeC estimated to run up inland with/without submerged seawalls

can be regarded as analogous to the backflows and modifications induced by the submerged seawalls. Together, these mechanisms-natural and artificial-play complementary roles in redistributing and dissipating tsunami energy before it reaches the shoreline.

Installation of hollow duct- and perforated-plate-type seawalls in a shallow coastal zone

When high-velocity tsunami currents enter the duct-type seawall, they generate a large vortex-rich backflow. Once this backflow is initiated within the duct, the through-flow effectively ceases. In the T-mCFT experiments, both the duct-type and perforated-plate-type submerged seawall models were set to approximately one-half of the water depth, with the porosity ratio of the plate designed at about two-thirds.

In the T-mCFT experiment, the models were constructed as rectangular parallelepipeds with a height-to-length ratio of roughly 1:4. Under these conditions, the duct-type model generated a backflow volume equivalent to 28.6% of the inflow, while the perforated-plate-type model produced 21.2% (Table 1). These results suggest that submerged seawalls can transform nearly half of the incoming tsunami current into backflow.

Based on these findings, Fig. 9 illustrates a proposed arrangement of hollow duct-type and hollow perforated-plate-type submerged seawalls, aligned parallel to the shoreline. In this configuration, seawalls approximately 3 m in height would be installed on the seabed at a depth of about 6 m, located approximately 600 m offshore.

As a more cost-effective alternative, the seawalls could be raised from 3 m to 4 m in height and positioned in shallower water, with seabed depth reduced from 6 m to 5 m. Installing the structures slightly closer to the shoreline is expected to provide protective performance comparable to that of the existing coastal wave breaker, while maintaining or even enhancing the effectiveness against both the surface SuWaF and the jet-like BeJeC.

Discussion

Natural examples of reduced destructive energy in low-layer jet currents (BeJeC) generated by megatsunamis include coral reefs, mangrove forests, and clusters of small islands.

With respect to the roughness and porosity of coral reefs (fringing and barrier types), both observational data and numerical simulations have demonstrated that the roughness of shallow reef flats and branching corals increases bottom friction, thereby reducing flow velocity and energy flux. After the 2004 Indian Ocean tsunami, an analysis around the Maldives reported that energy flux decreased in areas with high coral cover[7]. In idealized topographic models, barrier reefs located in shallow water within 1–2 meters of the sea surface were shown to reduce run-up on land by approximately

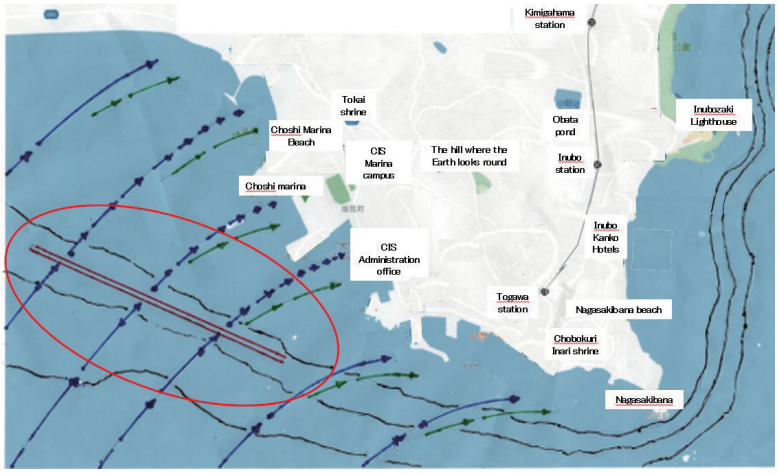

Fig. 9 Proposed configuration of duct-type and perforated-plate-type submerged seawalls for the shallow waters of Choshi Marina.

50%[8]. Other studies have indicated that porous coverage suppresses flow velocity as waves pass through it, thereby decreasing active inflow and inundation compared with uncovered conditions[9].

Mangrove forests provide another representative example of porous coastal natural structures. The reticulated structures formed by trunks, roots, and pneumatophores attenuate wave height, flow velocity, and force, thereby contributing to tsunami disaster risk reduction. Experiments using mangrove models have demonstrated reduced downstream velocity and force. However, mangroves face challenges such as site-specific growth conditions, long maturation periods, and the risk of destruction by megatsunamis. For this reason, they are often considered not as stand-alone countermeasures but as part of a "nature-based hybrid defense" in combination with engineered hard structures[10].

The scattering and refraction of waves caused by chains of small islands may also reduce tsunami energy, but depending on their configuration they may act as a "lens effect," concentrating energy on the leeward coast and amplifying run-up. Because this effect is highly dependent on geomorphology and local depth conditions, it cannot be generalized that "a greater number of islands always reduces tsunami impact."[11]

During the March 11, 2011, mega-tsunami, the Kashimanada coast of Ibaraki Prefecture was struck directly, suffering catastrophic damage that washed away massive headland groups and drastically reshaped the coastline. In contrast, the Byobugaura cliff system in Choshi City, Chiba Prefecture-featuring similar coastal forms and scale-experienced tsunami impact in a different manner. The tsunami struck the southernmost rock masses protruding from the cliff system. The frontal rock plate was fractured and displaced, but apart from this localized destruction, no extensive devastation was observed.

In the shallow coastal area east of Byobugaura, about 1 km offshore, a large tsunami current surged in and gradually elevated the sea surface until a sudden GW3 formed above it. This process consumed a considerable portion of the tsunami' s energy, illustrating how natural flow transformations also function as mechanisms of energy dissipation-similar in principle to the artificial backflows generated by submerged seawalls.

For countermeasure design, we therefore propose a double submerged seawall system in shallow waters near Choshi Marina. A duct-type seawall approximately 7 m in length could be positioned seaward, followed 15 m behind by a perforated-plate-type seawall of comparable length. When installed at seabed depths of 5–6 m and heights of 3–4 m, these structures would operate in conjunction with natural energy-dissipation processes (e.g., GW3 forma-tion) to reduce the destructive force of incoming mega-tsunamis and induce stable backflows toward the sea.

Acknowledgements: We would like to express our sincere gratitude to the staff of Chiba Institute of Science for their guidance and support in conducting the experiments using the T-mCFT. We are also grateful to the City of Choshi and the Choshi Fire Department for their valuable advice on tsunami countermeasures, which greatly contributed to defining the research direction of our group. Their insights were instrumental in the design and feasibility assessment of the submerged seawall models. We are especially indebted to Professor Emeritus Shinji Honami of Tokyo University of Science for his invaluable comments on our study of the destructive forces of supercritical tsunami flows and submerged seawalls-an area with very few prior investigations.

Conflict of interest: A.T., E.M., R.K, and Y.Y declare no conflict of interest.

References

1) Satake, K., Fujii, Y., Harada, T., Namegaya, Y: Time and space distribution of coseismic slip of the 2011 Tohoku earthquake as inferred from tsunami waveform data. Bull Seismol Soc Am 2013; 103:1473–1492.
2) Gusman, A. R., Tanioka, Y., Satake, K: Source model of the great 2011 Tohoku earthquake estimated from

tsunami waveforms and crustal deformation data. Earth Planet Sci Lett 2012; s341–344(4): 234–242.

3) Mas, E., Koshimura, S., Imamura, F., Suppasri, A., Muhari, A., Adriano, B: Recent advances in agent-based tsunami evacuation simulations: Case studies in Indonesia, Thailand, Japan and Peru. Pure Appl Geophys 2015; 172: 3409–3424.
4) Yeh, H., Sato, S., & Tajima, Y: The 11 March 2011 east Japan earthquake tsunami effects on coastal infrastructure and buildings. Pure Appl Geophys 2012; 170: 1019–1031.
5) Arikawa, T., Sato, M., Shimosako, K., Hasegawa, I., Yeom, G.-S., Tomita, T: Failure mechanism of Kamaishi breakwaters due to the great East Japan earthquake tsunami. Coast Eng Proc 2012; 1: 1–13.
6) Oetjen, J., Sundar, V., Venkatachalam, S., Reicherter, K., Engel, M., Schüttrumpf, H., Sannasiraj, S. A: A comprehensive review on structural tsunami countermeasures. Nat Hazards 2022; 113: 1419–1449.
7) Lahcene, E., Suppasri, A., Pakoksung, K., Imamura, F: The impact of the coral reef system on the tsunami propagation of the 2004 Indian Ocean event in North Male Atoll. Ocean Coast Manag 2024; 257: 107348.
8) Kunkel, C. M., Hallberg, R. W., Oppenheimer, M: Coral reefs reduce tsunami impact in model simulations. Geophys Res Lett 2006; 33, L23612, doi:10.1029/2006GL027892
9) Fernando, H.J.S., Samarawickrama, S., Balasubramanian, S., Hettiarachchi, S., Voropayev, S: Effects of porous barriers such as coral reefs on coastal wave propagation. J Hydro-environment Res 2008; 1: 187-194.
10) Benazir, B., Triatmadja, R., Syamsidik, S., Nizam, Warniyati, W: Vegetation-based approached for tsunami risk reduction: Insights and challenges. Prog Disaster Sci 2024; 23:100352
11) Rasyif, T. M., Kato, S., Syamsidik, S., Okabe, T: Influence of small islands against tsunami wave impact along Sumatra Island. J Jpn Soc Civ Eng SerB2(Coast Eng) 2016; 72: 331-336.